Photonic Crystals

International Edition: DOI: 10.1002/anie.201704801
German Edition: DOI: 10.1002/ange.201704801

Biologically Controlled Morphology and Twinning in Guanine Crystals

Anna Hirsch, Benjamin A. Palmer, Nadav Elad, Dvir Gur, Steve Weiner, Lia Addadi, Leeor Kronik,* and Leslie Leiserowitz**

Abstract: *Guanine crystals are widely used in nature as components of multilayer reflectors. Guanine-based reflective systems found in the copepod cuticle and in the mirror of the scallop eye are unique in that the multilayered reflectors are tiled to form a contiguous packed array. In the copepod cuticle, hexagonal crystals are closely packed to produce brilliant colors. In the scallop eye, square crystals are tiled to obtain an image-forming reflecting mirror. The tiles are about 1 μm in size and 70 nm thick. According to analysis of their electron diffraction patterns, the hexagon and square tiles are not single crystals. Rather, each tile type is a composite of what appears to be three crystalline domains differently oriented and stacked onto one another, achieved through a twice-repeated twinning about their ⟨011⟩ and ⟨021⟩ crystal axes, respectively. By these means, the monoclinic guanine crystal mimics higher symmetry hexagonal and tetragonal structures to achieve unique morphologies.*

Many organisms use guanine crystals to manipulate light in an astonishing variety of ways.[1,2] Guanine crystals are used to produce the white-matte color in certain spiders,[3,4] the metallic reflectance of fish,[5] and the brilliant iridescent colors of planktonic sapphirinid copepods[6,7] and tropical fish.[8,9] Some organisms can even reversibly tune their structural colors in response to illumination changes.[9–12] In some organisms, the different optical properties play a significant role in camouflage and display.[2,5,6] In others, guanine crystals are used for vision, that is, to collect, focus, and/or enhance light.[13] Organisms such as the *Pecten* scallop[14,15] and certain varieties of mesopelagic (deep-sea) fish[16,17] build complex guanine-based image-forming mirrors.

The optical properties of guanine are based on its high-index of refraction.[1] The white-matte color of some spiders is obtained by diffuse reflection of all wavelengths from block-shaped prismatic guanine crystals. In most other systems, optical properties are produced by interference of light reflected from alternating layers of thin guanine crystals and cytoplasm, corresponding to high and low refractive-index materials, respectively. Thus, the enormous variety in color, iridescence, and reflection is achieved by control of the arrangement, morphology, size, and structure of the guanine crystals.[18]

While the connection between guanine crystals and the reflectance of fish skin has been known for over 100 years,[19] the crystal structure of synthetic guanine (α polymorph) was determined only a decade ago[20] and that of biogenic guanine (β polymorph) was determined only two years ago.[21] It is noteworthy that for both polymorphs, the structure adopted by the guanine molecule is the N7-protonated tautomer.[20] The two polymorphs differ in the molecular stacking orientation but possess similar calculated lattice energies.[21] Nevertheless, all biogenic guanine samples examined to date exhibit the β form (as an example, X-ray diffraction data for the scallop are given in the Supporting Information, Figure S1). The β-guanine crystal structure has monoclinic symmetry, with a unique *c*-axis. The guanine molecules form perfectly H-bonded layers in the *bc* plane, which stack in the perpendicular *a** direction with a molecular offset along the *b*-axis, forming an anisotropic structure (Supporting Information, Figure S2 A,B).

The pronounced anisotropy expresses itself in the optical properties; while the measured refractive index parallel to the H-bonded layers is $n = 1.5$, the stacking direction has an extremely high measured refractive index of $n = 1.8$.[22] To optimize their reflectivity, many organisms exert exquisite control over crystal morphology. Whereas stable guanine crystals adopt a prismatic shape,[3,4,18] many organisms form plate-like single crystals in which the high refractive-index face is preferentially expressed.[23,24]

The sapphirinid copepod (*S. metallina*) and the *Pecten* scallop (*Pecten maximus*) exert additional control over the ultrastructural arrangement and morphology of their guanine crystals; the guanine crystals in each layer of the reflector are arranged in a contiguous manner, forming a perfectly tiled reflecting surface.[6,14] The copepods form an array of tiled stacks composed of thin hexagonal-shaped guanine crystals underneath their chitin cuticle, whereas the scallop eye mirror is composed of tiled stacks of square-shaped guanine crystal platelets (Figure 1 A,B). All tiles are about the same size and shape and are arranged such that sides of neighboring tiles

[*] A. Hirsch, Prof. L. Kronik, Prof. L. Leiserowitz
Department of Materials and Interfaces, Weizmann Institute of Science
Rehovoth 76100 (Israel)
E-mail: leeor.kronik@weizmann.ac.il
leslie.leiserowitz@weizmann.ac.il
Dr. B. A. Palmer, Prof. S. Weiner, Prof. L. Addadi
Department of Structural Biology, Weizmann Institute of Science
Rehovoth 76100 (Israel)
E-mail: lia.addadi@weizmann.ac.il
Dr. N. Elad
Department of Chemical Research Support, Weizmann Institute of Science
Rehovoth 76100 (Israel)
Dr. D. Gur
Departments of Molecular Cell Biology and of Physics of Complex Systems, Weizmann Institute of Science
Rehovoth 76100 (Israel)
Supporting information and the ORCID identification number(s) for the author(s) of this article can be found under: https://doi.org/10.1002/anie.201704801.

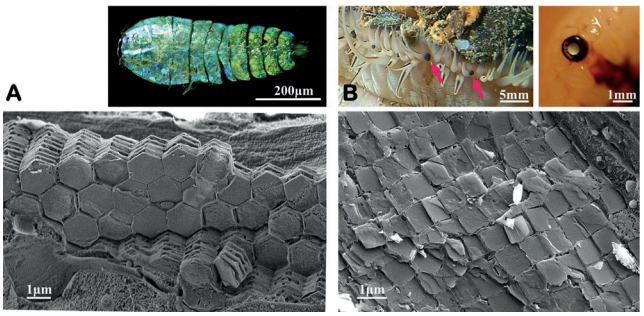

Figure 1. A) Top: Light microscopy image of *S. metallina* copepod. Bottom: Cryo-SEM image of the hexagonal guanine tiling covering the body of the organism. 12–13 hexagonal thin tiles are stacked on top of each other. B) Top left: Photograph of several eyes of a *P. maximus* scallop (which possesses up to 200 eyes) lining the mantle tissue. Pink arrows point to two of the eyes. Top right: Photograph of one eye. Bottom: Cryo-SEM of a congruent layer of square guanine tiles taken from the scallop eye. The mirror is constructed from a multilayer stack of 20–30 crystals, separated by thin layers of cytoplasm.

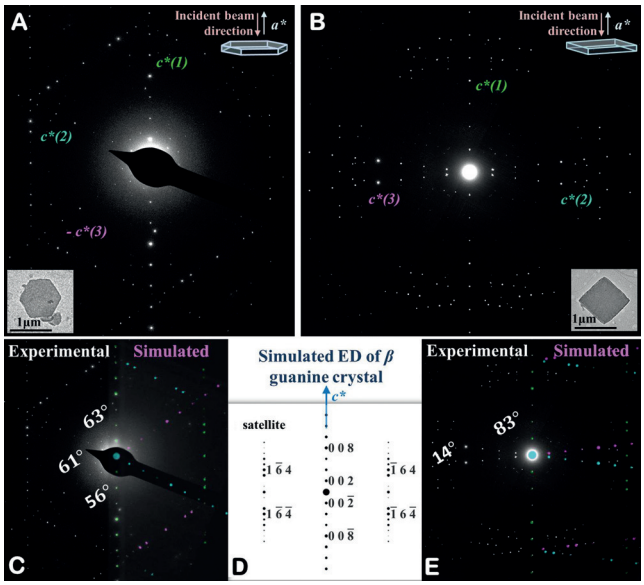

Figure 2. Observed ED patterns of A) a copepod-guanine crystal and a B) scallop-guanine crystal. In each ED pattern there are three diffraction rows crossing the center, each exhibiting d^* spacings corresponding to twice the c^* axis of β-guanine. A schematic of the TEM setup is shown in the upper right corner of each ED pattern, showing the incident electron beam direction perpendicular to the crystal plate and (anti-)parallel to the a^* axis. The morphology and orientation of the measured crystal is displayed at the bottom corner of each ED pattern. Comparison of the observed and simulated ED pattern of C) a copepod-guanine and E) a scallop-guanine crystal. The marked angles are average values measured from several (n) observed ED patterns. The angles are 63 ± 1°, 61 ± 1°, and 56 ± 2° for copepod-guanine (n = 13) and 83 ± 0.5° and 14 ± 0.2° for scallop-guanine (n = 15). Each simulated ED pattern is a superposition of three monoclinic crystal domains, with D) the simulated ED pattern of a single monoclinic crystal. In the simulated ED pattern, the differently colored diffraction rows originate from different domains. (To improve the visibility of different regions in the ED pattern of panels (A) and (B), images of a different contrast were combined, and in (B) all spots were highlighted simultaneously.)

match precisely,[25] with the arrangement repeating so as to cover a plane with almost no gaps or overlaps.

The angles between the lateral faces of the copepod crystals are 120 ± 3° and in the scallop crystals they are 90 ± 3°; that is, regular hexagons and squares are produced, respectively. In formal symmetry terms, the point groups of the hexagonal and square morphologies are 6/*mmm* and 4/*mmm*, respectively (Supporting Information, Table S1). Surprisingly, these high-symmetry morphologies are produced from a crystal with the lower symmetry point group (2/*m*) of the β-guanine.

To resolve this conundrum, we performed electron diffraction (ED) measurements on copepod and scallop guanine single crystals. Figure 2 shows typical ED patterns of the hexagonal (copepod) and square (scallop) crystals, with the corresponding morphological orientations (Figure 2 A,B). The ED patterns were obtained by electron beam irradiation perpendicular to the face of the crystal, and thus (anti-) parallel to the a^* axis of the crystals (upper right corners in Figure 2 A,B). The three diffraction rows, crossing the center of each pattern, exhibit d^* spacings and intensities equal to those of the (00l) row of monoclinic β guanine (Figure 2 D). This assignment is reinforced by the presence of satellite diffraction rows on opposite sides of the central row, which perfectly match the calculated satellite reflections (Figure 2 D and Supporting Information, Figures S2 C,D and S3).

The presence of the three (00l, $l = 2n$) diffraction rows with similar intensities implies that the hexagon and square crystals, both with a total thickness of circa 70 nm, are not single crystals. Rather, they are a composite of what appears to be three crystal domains with different orientations. Selected-area ED of different areas of individual copepod- and scallop-guanine crystals yielded diffraction patterns similar to those of the whole crystal, implying that each domain covers the whole crystal face area (Supporting Information, Figures S4 and S5). The angles between these crystal domains correspond to those measured between the (00l) electron diffraction rows in Figure 2 C,E. Indeed, we could reproduce the observed ED patterns of copepod- and scallop-guanine crystals by making use of the measured azimuthal angles between the (00l) diffraction rows, as shown in Figure 2 C,E. On cursory inspection, the copepod-guanine ED pattern exhibits 6/*mmm* point symmetry, in keeping with the hexagonal morphology of the crystal. A detailed analysis reveals small deviations from regular 60° angles. The deviation from ideal morphology is even more pronounced in scallop-guanine crystals. The angle between two of the (00l) diffraction rows is 14°, but the angle between their bisectrix and the third (00l) row is 90°.

To achieve a regular hexagon or square crystal of monoclinic guanine, the six or the four side faces should be at least structurally equivalent. The {011} faces are stable according to the calculated theoretical morphology.[18] The angle between the {001} and the {011} planes is of 117.9° as projected onto the *bc* plane. A {100} plate delimited by two {001} and four {011} lateral faces would therefore have a slightly distorted hexagonal morphology (Figure 3A_1). To generate a regular hexagon crystal with six equivalent side faces we invoke a molecular interlayer twinning mechanism

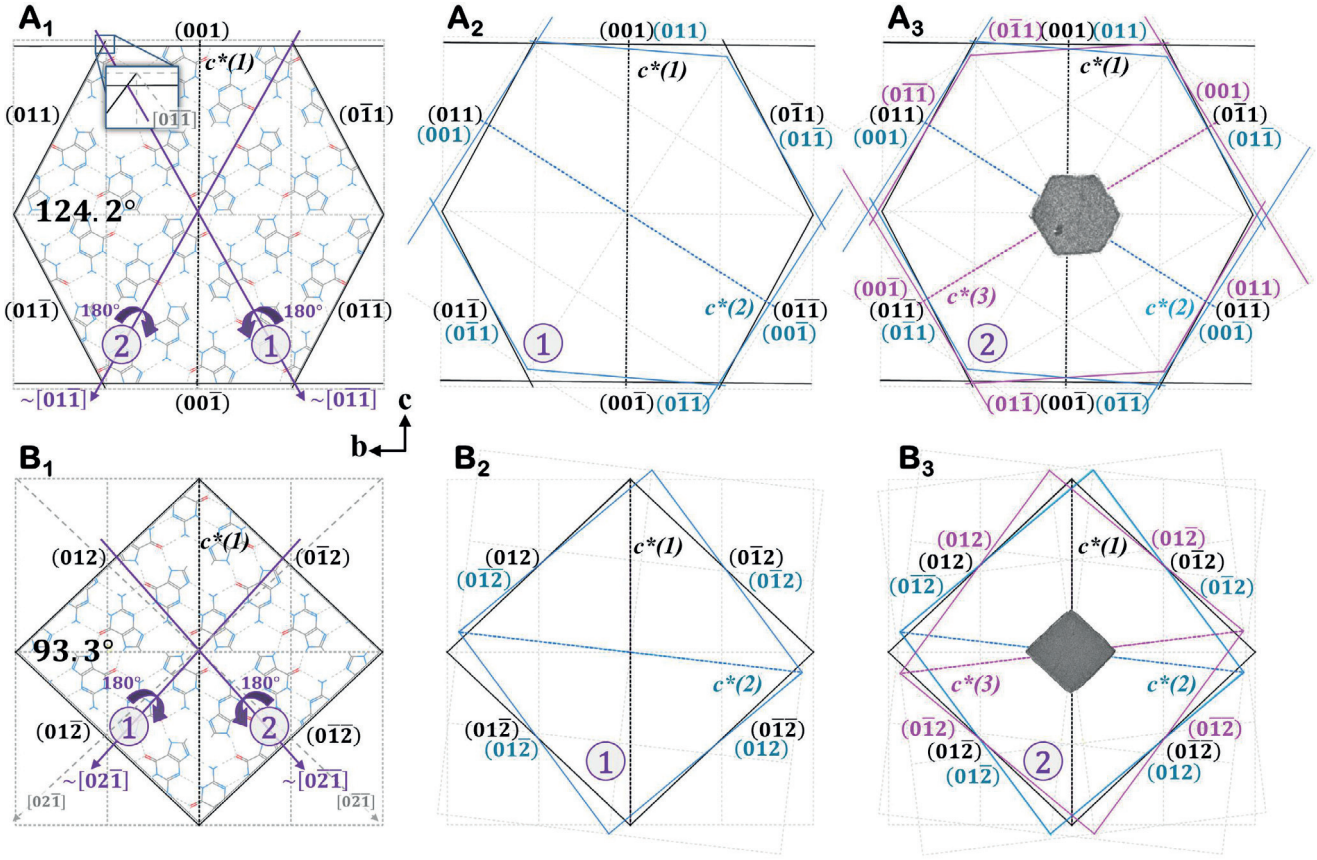

Figure 3. Illustration of the proposed guanine molecular interlayer twinning mechanism of the copepod (row A) and the scallop (row B) crystals. The model is illustrated for the monoclinic guanine *bc* layer. A_1) For the copepod, an irregular hexagonal shape is formed by six side faces; two of {001} and four of {011} planes. The enclosed projected angle onto the *bc* plane is 117.9° between the {011} and {001} edges and 124.2° between the {011} and {01$\bar{1}$} edges. The first rotational twinning operation of 180° is about the [0$\bar{1}\bar{1}$] crystal diagonal and the second operation about the alternative [01$\bar{1}$] diagonal (numbered and marked in purple in A_1). The twinning axes (in purple) are almost the crystallographic directions as shown in the insert. A_2) Once twinned, the second crystallite does not superimpose precisely onto the first one. A_3) The significant overlap of the three domains is complemented by the fit between the observed and simulated *c**(00*l*) directions. B_1) The twinning principle of the scallop-guanine is similar. A regular rhombus is delineated by four side faces with {012} edges, which enclose projected angles of 93.3° and 86.7°. The two twinning operations are about the [02$\bar{1}$] and the [0$\bar{2}\bar{1}$] crystal directions (numbered and marked in purple in B_1). B_2) Once twinned, the second crystallite does not superimpose precisely on the first one. The twinning axes (in purple) are almost the crystallographic directions, which are shown by the dashed gray line. B_3) The significant overlap of the three domains is complemented by the fit between the observed and simulated *c**(00*l*) directions.

about the [0$\bar{1}\bar{1}$] diagonal, which superimposes a projection of the {011} face on the {001} face. Once twinned, the second domain does not superimpose precisely on the first one (Figure 3A_2) because the twinning axis is not a perfect bisectrix between the two connecting {001} and {011} face edges (inset of Figure 3A_1). To make all side faces equivalent we invoke a second twinning operation about the alternative crystal diagonal [01$\bar{1}$] (Figure 3$A_{1,3}$), generating six equivalent side faces, each composed of layers of {001} and {011} faces. Through this procedure, we obtain an excellent fit between the orientation of the {001} crystal faces and the three observed (00*l*) diffraction rows, each of which is perpendicular to a pair of {001} faces.

To simulate the crystal shape of scallop-guanine, we consider the crystal morphology of fish guanine, which is a {100} thin hexagon elongated along the *b*-axis and delineated by two {001} side faces and four {012} end faces.[23] We replace this crystal by a {100} plate-like rhombus, delineated only by four {012} faces, which is almost square, given that the angle between the adjacent side {012} faces as projected onto the *bc* plane is 93.3° or 86.7°. The four side faces are structurally equivalent, but such a hypothetical morphology would not be formed normally, since the growth rates along the two diagonals of the rhombus corresponding to the *b* and *c* axes are significantly different, as exemplified by the fish-guanine morphology[18,23] (see also Supporting Information, Figure S6). We therefore rationalize the square scallop morphology by applying the principle of two-twinning operations (see above) about the [02$\bar{1}$] and [0$\bar{2}\bar{1}$] directions, respectively, to generate three crystal domains (Figure 3B). This creates an angle of $\pm 83°$ ($=2\times41.5°$) between the observed diffraction vectors *c**(1) and *c**(2) (or *c**(3)), which is reasonably close to 90°. Again, the twinned domains do not superimpose precisely onto the original one (Figure 3B_2) because the twinning axis is not precisely the ideal one (Figure 3B_1). Most importantly, the twinning alters the

directions of the *b* and *c* axes in adjacent crystal domains, thereby tending to homogenize growth rates so as to conform to the tile shape. This model, summarized in Figure 3, is supported by comparing geometrical scaled models with edge-on cryo-SEM images of the twinned crystal morphologies (Figure 4).

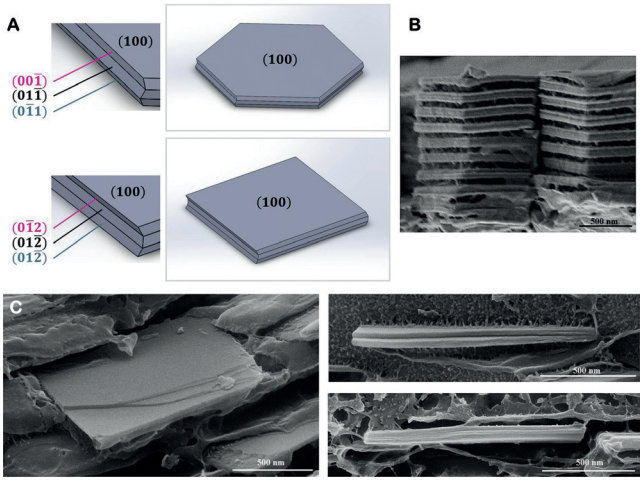

Figure 4. A) Scaled geometrical models of the twinned hexagon and square crystal morphologies of copepod- and scallop-guanine crystals, respectively, viewed approximately isometrically. These two crystals are not single crystals. Rather, each is a composite of what appears to be three stacked domains that are differently oriented. Of the different side faces of the two composite crystals, only {001} makes a dihedral angle of 90° with the plate-like (100) face. The {011} side faces of the hexagon and the {012} side faces of the square form dihedral angles of 63.5° and 68.8° with the (100) face, respectively. Cryo-SEM images of B) the hexagon and C) the square crystals viewed edge-on. The different domains of each composite are evident. In (C), the dominant crystal domains in the left panel were fractured, exposing the interface between them.

The biological function of the guanine crystals is different in the two organisms but in both it strongly depends on a contiguous arrangement of individual multilayer reflector tiles. In the copepod, the hexagonal tiling fully covers its cuticle. This allows simultaneous reflection (or lack thereof), which combined with spiral swimming allows for signaling through blinking or camouflage.[6] In the scallop, the square tiles are organized in a hierarchical structure that forms a focusing mirror, essential for forming a retinal image.[14] Crystal tiling produces a smoothly reflective surface by minimizing crystal interface defects that would cause optical diffraction and reduce the image contrast. However, as noted, achieving regular polygon tiling from an underlying monoclinic crystal symmetry poses a significant challenge. It has been overcome by three orientations of crystalline domains, employing a two-twinning principle about the *bc* H-bonded layer. This occurred in two very different organisms, suggesting convergent evolution. What makes this possible is an inherent property of the layered guanine structure, which allows the formation of irregular hexagon and regular rhombus morphologies (Figure 3) with stable faces delineated by low (0*kl*) indices exhibiting relatively smooth molecular surfaces. The general principle that drives the formation of regular shapes, then, is that their side faces are structurally equivalent, facilitating a similar growth rate.

Crystallographic twinning is not uncommon in biomineralization, occurring in a variety of crystals, including calcium carbonates,[26–28] calcium oxalates,[29] and magnetite.[30] Twinning was even observed in guanine from the white widow spider.[4] Formally, both copepod and scallop twinning can be considered to be mimetic, that is, simulating a higher crystal symmetry by morphology.[31] The twinning is almost of the "crystallographic orientation relation" type (see the Supporting Information),[31,32] with the "almost" referring to the non-ideal angles between the diffraction vectors. Unlike the twinning described in the white widow spider,[4] in the systems described herein the lattice registry between the twinned crystal domains is very limited. Indeed, this limited registry suggests that twinning is a consequence of another phenomenon, driven by the interplay between biological control and crystal structure properties. This biological control is striking, in that it enforces formation of perfectly stacked and oriented tiles with equal size and shape, each a composite of three crystal domain types. It is therefore conceivable that biological control can already be prevalent at the molecular level.

In conclusion, we characterized the unique hexagon and square shapes of the copepod and scallop guanine crystal tiles. We determined, based primarily on an analysis of the ED data, coupled with utilizing knowledge of the molecular packing arrangement and morphology of β-guanine, that the hexagon and square shapes may be achieved through a crystal twinning mechanism. This twinning appears to be controlled biologically. The precise mechanism of control remains a fascinating open question.

Acknowledgements

We thank Peter Rez and Sharon Wolf for useful discussions. This work was supported by the Israel Science Foundation. B.A.P. is the recipient of a Human Frontiers Cross-Disciplinary Postdoctoral Fellowship. L.A. and S.W. are the incumbents of the Dorothy and Patrick Gorman Professorial Chair of Biological Ultrastructure and the Dr. Trude Burchardt Professorial Chair of Structural Biology, respectively. Electron microscopy studies were supported in part by the Irving and Cherna Moskowitz Center for Nano and Bio-Nano Imaging. Our work was additionally supported by the historical generosity of the Perlman family.

Conflict of interest

The authors declare no conflict of interest.

Keywords: crystal twinning · electron diffraction · morphological engineering · photonic crystals · tiling

How to cite: *Angew. Chem. Int. Ed.* **2017**, *56*, 9420–9424
Angew. Chem. **2017**, *129*, 9548–9552

[1] M. F. Land, *Prog. Biophys. Mol. Biol.* **1972**, *24*, 75 – 106.
[2] P. J. Herring, *Comp. Biochem. Physiol. Part A* **1994**, *109*, 513 – 546.
[3] G. S. Oxford in *Proc. 17th Eur. Colloq. Arachnol. Edinb.* **1997**, pp. 121 – 131.
[4] A. Levy-Lior, E. Shimoni, O. Schwartz, E. Gavish-Regev, D. Oron, G. Oxford, S. Weiner, L. Addadi, *Adv. Funct. Mater.* **2010**, *20*, 320 – 329.
[5] E. J. Denton, *Philos. Trans. R. Soc. London Ser. B* **1970**, *258*, 285 – 313.
[6] J. Chae, S. Nishida, *Mar. Biol.* **1994**, *119*, 205 – 210.
[7] D. Gur, B. Leshem, M. Pierantoni, V. Farstey, D. Oron, S. Weiner, L. Addadi, *J. Am. Chem. Soc.* **2015**, *137*, 8408 – 8411.
[8] J. N. Lythgoe, J. Shand, *J. Physiol.* **1982**, *325*, 23.
[9] D. Gur, B. A. Palmer, B. Leshem, D. Oron, P. Fratzl, S. Weiner, L. Addadi, *Angew. Chem. Int. Ed.* **2015**, *54*, 12426 – 12430; *Angew. Chem.* **2015**, *127*, 12603 – 12607.
[10] G. S. Oxford, R. G. Gillespie, *Annu. Rev. Entomol.* **1998**, *43*, 619 – 643.
[11] J. Teyssier, S. V. Saenko, D. van der Marel, M. C. Milinkovitch, *Nat. Commun.* **2015**, *6*, 6368.
[12] D. Gur, B. Leshem, V. Farstey, D. Oron, L. Addadi, S. Weiner, *Adv. Funct. Mater.* **2016**, *26*, 1393 – 1399.
[13] M. F. Land, D.-E. Nilsson, *Animal Eyes*, Oxford University Press, Oxford, **2012**.
[14] M. F. Land, *J. Exp. Biol.* **1966**, *45*, 433 – 447.
[15] V. C. Barber, E. M. Evans, M. F. Land, *Z. Zellforsch. Mikrosk. Anat.* **1967**, *76*, 295 – 312.
[16] H.-J. Wagner, R. H. Douglas, T. M. Frank, N. W. Roberts, J. C. Partridge, *Curr. Biol.* **2009**, *19*, 108 – 114.
[17] J. C. Partridge, R. H. Douglas, N. J. Marshall, W.-S. Chung, T. M. Jordan, H.-J. Wagner, *Proc. R. Soc. London Ser. B* **2014**, *281*, 20133223.
[18] D. Gur, B. A. Palmer, S. Weiner, L. Addadi, *Adv. Funct. Mater.* **2017**, *27*, 1603514.
[19] J. T. Cunningham, C. A. MacMunn, *Proc. R. Soc. London* **1893**, *53*, 384 – 388.
[20] K. Guille, W. Clegg, *Acta Crystallogr. Sect. C* **2006**, *62*, o515 – o517.
[21] A. Hirsch, D. Gur, I. Polishchuk, D. Levy, B. Pokroy, A. J. Cruz-Cabeza, L. Addadi, L. Kronik, L. Leiserowitz, *Chem. Mater.* **2015**, *27*, 8289 – 8297.
[22] W. J. Schmidt, *Giess. Naturwissenschaft. Vortr.* **1949**, *6*, 1 – 71.
[23] A. Levy-Lior, B. Pokroy, B. Levavi-Sivan, L. Leiserowitz, S. Weiner, L. Addadi, *Cryst. Growth Des.* **2008**, *8*, 507 – 511.
[24] T. M. Jordan, J. C. Partridge, N. W. Roberts, *Nat. Photonics* **2012**, *6*, 759 – 763.
[25] B. Grunbaum, G. C. Shephard, *Tilings and Patterns*, New York, W. H. Freeman, **1987**.
[26] M. E. Marsh, R. L. Sass, *Science* **1980**, *208*, 1262 – 1263.
[27] J. Liu, M. Sarikaya, I. A. Aksay, *MRS Proc.*, Cambridge Univ Press, **1991**, p. 9.
[28] M. Suzuki, H. Kim, H. Mukai, H. Nagasawa, T. Kogure, *J. Struct. Biol.* **2012**, *180*, 458 – 468.
[29] A. M. Cody, H. T. Horner, *Am. J. Bot.* **1985**, *72*, 1149 – 1158.
[30] B. Devouard, M. Posfai, X. Hua, D. A. Bazylinski, R. B. Frankel, P. R. Buseck, *Am. Mineral.* **1998**, *83*, 1387 – 1398.
[31] T. Hahn, H. Klapper, *International Tables for Crystallography*, International Union Of Crystallography, Chester, **2006**, pp. 393 – 448.
[32] F. C. Phillips, *An Introduction to Crystallography*, Longman Higher Education, Harlow, Essex, **1977**.

Manuscript received: May 10, 2017
Accepted manuscript online: June 18, 2017
Version of record online: July 6, 2017

